




Influence of Co and Al on Magnetic Properties and Magnetocaloric Effect of (Ni, Co)-Mn-(Sn, Al) Alloys

KIEU XUAN HAU ^{1,2,6} VU MANH QUANG,^{3,4} NGUYEN THI MAI,⁵
NGUYEN HAI YEN,¹ PHAM THI THANH,¹ TRAN DANG THANH,^{1,4}
PHAM DUC HUYEN YEN,² DONG HYUN KIM,² SEONG CHO YU,^{2,7}
and NGUYEN HUY DAN^{1,4}

1.—Institute of Materials Science, Vietnam Academy of Science and Technology, 18 Hoang Quoc Viet, Ha Noi, Viet Nam. 2.—Chungbuk National University, Cheongju 361 - 763, South Korea. 3.—Hanoi Pedagogical University No. 2, 32 Nguyen Van Linh, Xuan Hoa, Phuc Yen, Vinh Phuc, Viet Nam. 4.—Graduate University of Science and Technology, Vietnam Academy of Science and Technology, 18 Hoang Quoc Viet, Ha Noi, Viet Nam. 5.—College of Printing Industry, Phuc Dien, Bac Tu Liem, Ha Noi, Viet Nam. 6.—e-mail: kieuquanhou0106@gmail.com. 7.—e-mail: scyu@chungbuk.ac.kr

This paper investigates the influence of Co and Al concentrations on the structure, magnetic properties and magnetocaloric effect of (Ni, Co)-Mn-(Sn, Al) alloy ribbons prepared by melt-spinning. X-ray diffraction analyses show multi-crystalline phase characteristic of the ribbons including face-centered cubic ($L1_0$), body-centered cubic (B2), orthorhombic (4O) and monoclinic (10M) phases. The amplitude and temperature of the martensite–austenite phase transition of the alloy clearly depend on Co and Al concentrations. Magnetization measurements reveal soft magnetic features, with coercivity less than 50 Oe for all the alloy ribbons. The Curie temperature of the austenite phase increases with increasing Co concentration, but decreases with increasing Al concentration. The magnetic phase transitions in the alloy can be shifted to the room temperature region by adjusting the Co and Al concentrations. With appropriate concentrations of Co and Al, the alloy ribbons possess both negative and positive magnetocaloric effects, with a maximum magnetic entropy change larger than $0.6 \text{ J kg}^{-1} \text{ K}^{-1}$ in a magnetic field change of 12 kOe. The temperature and magnetic field dependence of the magnetocaloric effect in these alloy ribbons was also investigated.

Key words: Magnetocaloric effect, Heusler alloy, rapidly quenched alloys, phase transitions, Curie temperature, magnetic refrigeration

INTRODUCTION

The magnetocaloric effect (MCE) is the heating or cooling of a body when it is placed in or taken out of a magnetic field. This effect can be applied to magnetic refrigeration technology, as it offers the advantage of energy savings and is environmentally friendly.^{1–6} One potential type of magnetocaloric materials is Heusler alloys, among which the Ni-Mn-Sn alloy system has been attracting the

attention of scientists, because these alloys reveal a giant magnetocaloric effect (GMCE). Importantly, the Ni-Mn-Sn Heusler alloys exhibit both negative and positive GMCEs. The former is caused by the martensitic–austenitic structural transformation, and the latter is related to the ferromagnetic–paramagnetic phase transition.^{7–12} For high-efficiency magnetic refrigeration, magnetocaloric materials should possess high magnetic entropy change (ΔS_m) and large adiabatic temperature variation (ΔT_{ad}). A requirement for practical applications of household appliances is that the magnetocaloric materials have magnetic phase transitions at the room temperature region.^{13–22} The results of recent

studies showed that the addition of Co and Al can strongly affect the structural transformation and magnetic properties of the Ni-Mn-Sn Heusler alloy system. Partial substitution of Co atoms for Ni sites in the Ni-Mn-Sn alloys results in a significantly increased magnetization change at the martensitic–austenitic transformation (ΔM). This large change in magnetization greatly enhances the MCE for the alloys.^{23,24} The results also indicate that the transformation temperature of the martensitic–austenitic phases decreases gradually while the Curie temperature increases significantly with increasing concentration of Co. Thus, the substitution of Co for Ni can significantly improve the exchange interactions in alloys. As for the substitution of Al for Sn, the transformation temperature of martensitic–austenitic phases is affected more strongly than the Curie temperature of the austenitic phase.^{25–27} The martensitic–austenitic structural transformation of the (Ni, Co)-Mn-(Sn, Al) bulk alloys was found to be very sensitive to crystalline phases and concentrations of Co and Al. The crystalline phases of these types of Heusler alloys could be stabilized by an annealing process. However, it commonly takes a long time (up to several days) to make structural phases stable.^{28–30} To avoid the long annealing process, some research groups fabricated the Heusler alloys in ribbon form by rapid quenching. In comparison with bulk samples of the same

composition, the alloy ribbons exhibit a different crystalline structure and magnetic properties. The martensitic–austenitic transformation temperature in $\text{Ni}_{50-x}\text{Co}_x\text{Mn}_{31+y}\text{Al}_{19-y}$ ($x = 5, 10$) ribbon alloys is considerably lower than that of the bulk alloys, resulting in the difference in magnetic phase transitions. The $\text{Ni}_{50}\text{Mn}_{37}\text{Sn}_{13}$ and $\text{Ni}_{45}\text{Co}_5\text{Mn}_{32}\text{Al}_{18}$ alloy ribbons were found to exhibit a clear martensitic–austenitic transformation. The $\text{Ni}_{50-x}\text{Co}_x\text{Mn}_{31+y}\text{Al}_{19-y}$ ($x = 5, 10$) alloy ribbons show much stronger ferromagnetic behavior than the $\text{Ni}_{50}\text{Mn}_{31}\text{Al}_{19}$ ribbons.^{31–36}

In this work, we investigated the influence of Co and Al concentrations on the structure, magnetic properties and magnetocaloric effect of (Ni, Co)-Mn-(Sn, Al) alloy ribbons prepared by rapid quenching.

EXPERIMENT

For sample preparation, bulk alloys with nominal composition of $\text{Ni}_{50-x}\text{Co}_x\text{Mn}_{37}\text{Sn}_{13}$ ($x = 0, 2, 4, 6, 8,$ and 10) and $\text{Ni}_{50-x}\text{Co}_x\text{Mn}_{50-y}\text{Al}_y$ ($x = 5, 6, 7, 8, 9$ and 10 ; $y = 18$ and 19) were first fabricated from elements Ni, Co, Mn, Sn and Al of 99.9% purity using an arc-melting furnace. The resulting bulk alloys were then used to fabricate the alloy ribbons using a melt-spinning method on a single roller system. A tangential velocity of 40 m/s was applied to the copper roller to obtain ribbons with thickness

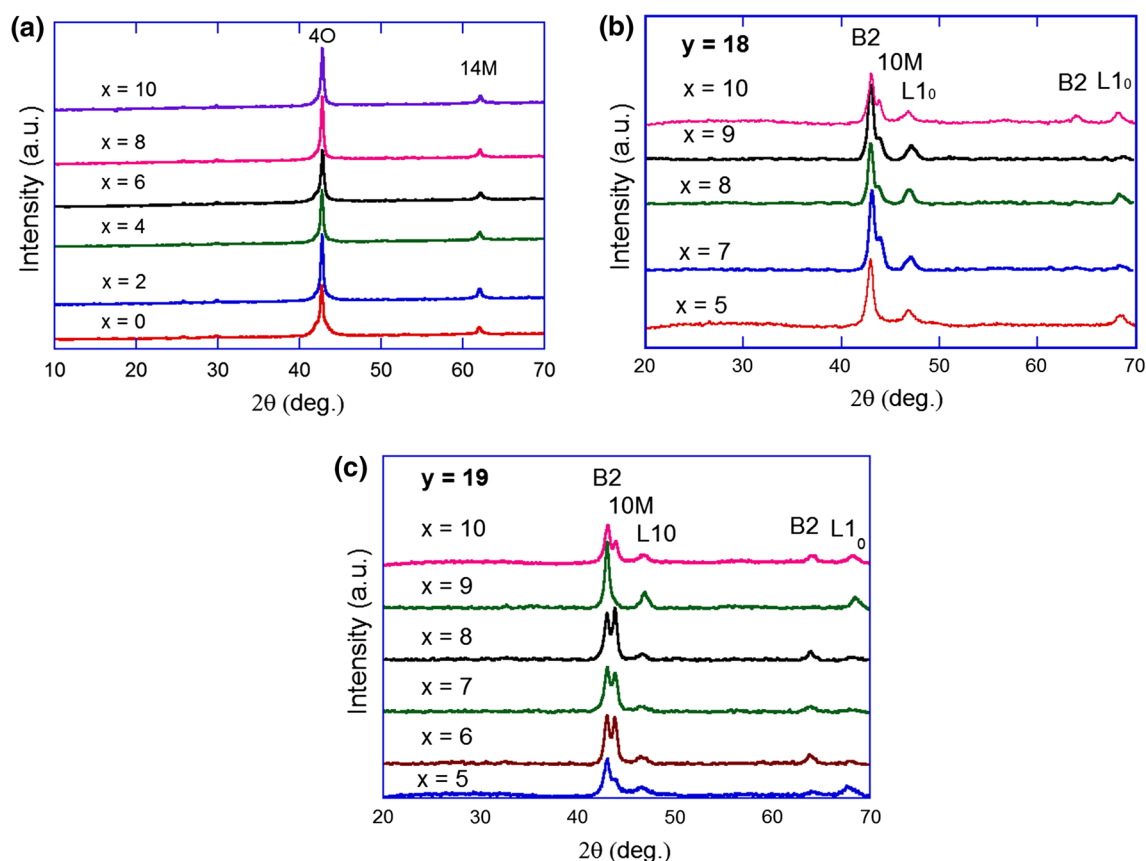


Fig. 1. XRD patterns of $\text{Ni}_{50-x}\text{Co}_x\text{Mn}_{37}\text{Sn}_{13}$ (a) and $\text{Ni}_{50-x}\text{Co}_x\text{Mn}_{50-y}\text{Al}_y$ with $y = 18$ (b) and 19 (c) ribbons.

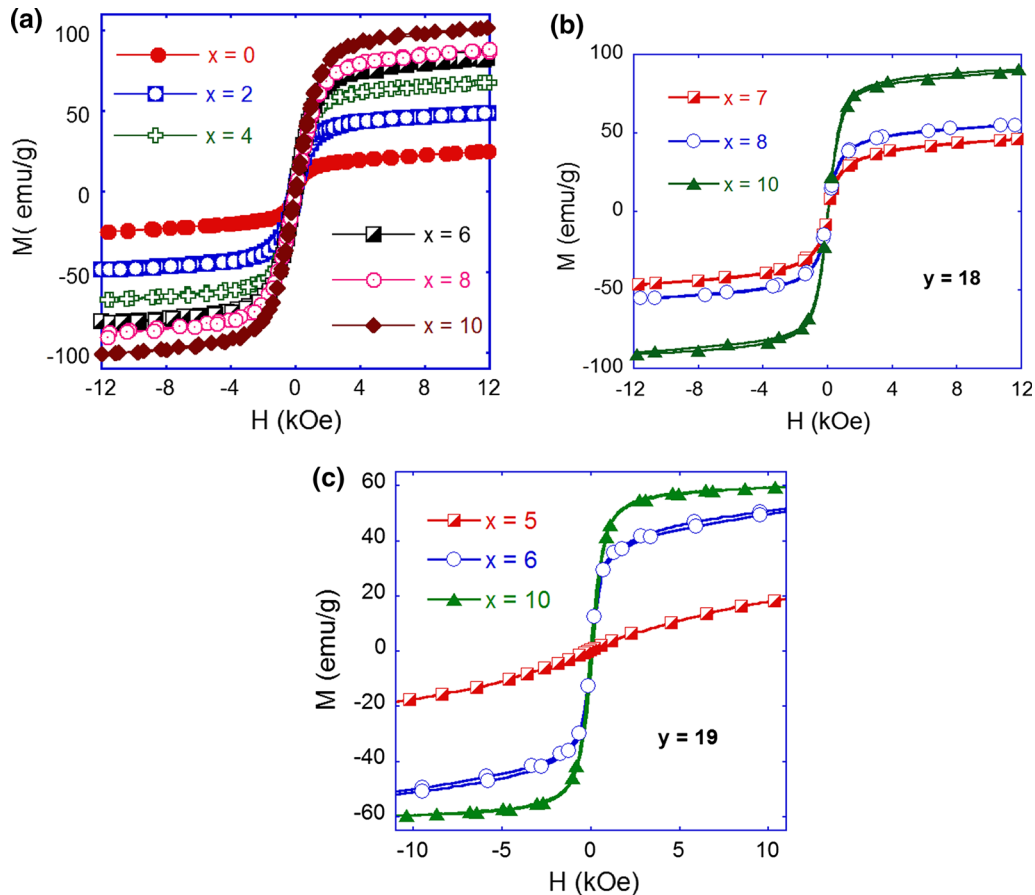


Fig. 2. Hysteresis loops of $\text{Ni}_{50-x}\text{Co}_x\text{Mn}_{37}\text{Sn}_{13}$ (a) and $\text{Ni}_{50-x}\text{Co}_x\text{Mn}_{50-y}\text{Al}_y$ with $y = 18$ (b) and 19 (c) ribbons.

of about $15\ \mu\text{m}$. To avoid oxidization, all the arc-melting and melt-spinning processes were performed under an argon atmosphere. As for sample characterization, the crystalline structure of the fabricated alloy ribbons was examined by powder X-ray diffraction (XRD) with Cu-K_α radiation ($\lambda = 1.54060\ \text{\AA}$) in 2θ ranging from 10° to 70° . The magnetic properties of the alloy ribbons were investigated on a vibrating-sample magnetometer (VSM) with a magnetic field range of $-12\ \text{kOe}$ to $12\ \text{kOe}$. The measurement temperature of the VSM could be changed from nitrogen liquid temperature up to $500\ \text{K}$. The magnetocaloric effects of the alloy ribbons were assessed from the magnetization data obtained.

RESULTS AND DISCUSSION

The XRD patterns of the $\text{Ni}_{50-x}\text{Co}_x\text{Mn}_{37}\text{Sn}_{13}$ and $\text{Ni}_{50-x}\text{Co}_x\text{Mn}_{50-y}\text{Al}_y$ ($y = 18$ and 19) alloy ribbons measured at room temperature are presented in Fig. 1. The multi-crystalline phase behavior of the ribbons is clearly dependent on the concentrations of Co and Al. One can see that the characteristic patterns of the $\text{Ni}_{50-x}\text{Co}_x\text{Mn}_{37}\text{Sn}_{13}$ and $\text{Ni}_{50-x}\text{Co}_x\text{Mn}_{50-y}\text{Al}_y$ ribbons are quite different. The $\text{Ni}_{50-x}\text{Co}_x\text{Mn}_{37}\text{Sn}_{13}$ XRD patterns show a multi-phase structure of 4O (orthorhombic) and 14M

(monoclinic), while the diffraction peaks on the XRD patterns of $\text{Ni}_{50-x}\text{Co}_x\text{Mn}_{50-y}\text{Al}_y$ are identified as belonging to the crystalline phases of B2 (body-centered cubic), L1_0 (face-centered cubic) and 10M (monoclinic). The structure of the $\text{Ni}_{50-x}\text{Co}_x\text{Mn}_{37}\text{Sn}_{13}$ ribbons is nearly unchanged when the Co concentration is increased from 0% to 10% (see Fig. 1a). As for the $\text{Ni}_{50-x}\text{Co}_x\text{Mn}_{50-y}\text{Al}_y$ ($y = 18$ and 19) ribbons, the quantity of the diffraction peaks tends to increase with Co concentration (see Fig. 1b and c). When the Al concentration increases, the 10M peak is dominant. It should be noted that the magnetic properties of these types of Heusler alloys are very sensitive to their structure. A small change in the structure of the $\text{Ni}_{50-x}\text{Co}_x\text{Mn}_{37}\text{Sn}_{13}$ and $\text{Ni}_{50-x}\text{Co}_x\text{Mn}_{50-y}\text{Al}_y$ alloy ribbons can greatly affect their magnetic properties. The effect of structure on the magnetic properties of the alloy ribbons will be presented in detail below.

The magnetic properties of the alloy ribbons were investigated by hysteresis and thermal magnetization measurements. Figure 2 shows the hysteresis loops of the $\text{Ni}_{50-x}\text{Co}_x\text{Mn}_{37}\text{Sn}_{13}$ and $\text{Ni}_{50-x}\text{Co}_x\text{Mn}_{50-y}\text{Al}_y$ ($y = 18$ and 19) ribbons. One can see that all the ribbons reveal soft magnetic behavior with low coercivity smaller than $50\ \text{Oe}$. This is a requirement for magnetic refrigeration

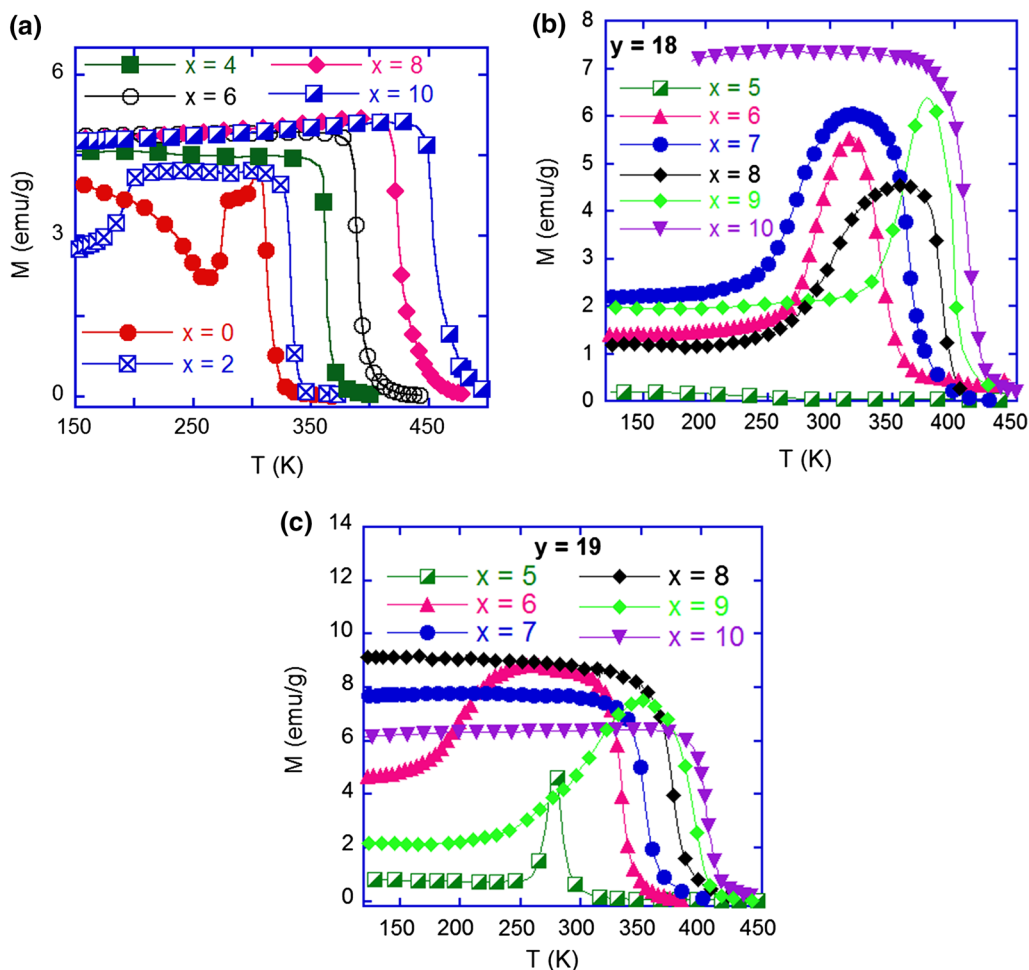


Fig. 3. Thermomagnetization curves in $H = 100$ Oe of $\text{Ni}_{50-x}\text{Co}_x\text{Mn}_{37}\text{Sn}_{13}$ (a) and $\text{Ni}_{50-x}\text{Co}_x\text{Mn}_{50-y}\text{Al}_y$ with $y = 18$ (b) and 19 (c) ribbons.

applications, because the thermal and magnetic hysteresis losses should be small or negligible. When the Co concentration increases, the saturation magnetization of the alloy ribbons is greatly enhanced, while an increase in the Al concentration causes this value to decrease. As Al is a non-ferromagnetic element, the magnetization of the alloys is reduced by increasing its concentration. Our results are in good agreement with those reported elsewhere.³⁷

In order to investigate the phase transitions of the $\text{Ni}_{50-x}\text{Co}_x\text{Mn}_{37}\text{Sn}_{13}$ and $\text{Ni}_{50-x}\text{Co}_x\text{Mn}_{50-y}\text{Al}_y$ ($y = 18$ and 19) ribbons, their thermo-magnetization curves in magnetic field $H = 100$ Oe were performed (Fig. 3). As reported, the Ni-Mn-Sn Heusler alloys exhibit two types of magnetic phase transitions, one related to the structural transformation from martensite to austenite (first-order phase transition), and the other due to the magnetic order change from ferromagnetic to paramagnetic (second-order phase transition).³¹⁻³³ Normally, the austenitic phase has strong ferromagnetic orders, while the martensitic phase is associated with weak ferromagnetic or antiferromagnetic couplings.³⁸⁻⁴⁰ As shown in Fig. 3, the shape of the

thermomagnetization curves clearly depends on both the Co and Al concentrations. Some samples exhibit both types of phase transitions. The first-order phase transition occurs at a martensitic-austenitic structural transition temperature (T_{MA}^{A}), and the second-order phase transition occurs at the Curie temperature of the martensitic phase (T_{C}^{M}) or austenitic phase (T_{C}^{A}). The T_{C}^{A} of the alloy ribbons strongly increases with increasing concentration of Co, while the concentration of Al clearly influences the martensitic-austenitic structural transformation temperature. The T_{C}^{A} of the $\text{Ni}_{50-x}\text{Co}_x\text{Mn}_{37}\text{Sn}_{13}$ ribbons is increased from ~ 314 K to ~ 456 K as the Co concentration increases from 0% to 10% (see Fig. 3a). The T_{C}^{M} is only observed on the sample with $x = 0$, at ~ 250 K, and a weak martensitic-austenitic transformation (at ~ 200 K) still remains on the sample with $x = 2$. This means that Co causes the martensitic phase to dominate in the alloy. As for $\text{Ni}_{50-x}\text{Co}_x\text{Mn}_{50-y}\text{Al}_y$ ribbons, the thermomagnetization curves of the alloy ribbons with $y = 18$ (Fig. 3b) show that the first-order magnetic phase transition occurs when the Co concentration is in the range of 6% to 9%. The T_{MA}^{A} is raised from ~ 282 K (for $x = 7$) to ~ 380 K (for $x = 9$). This transition is absent in

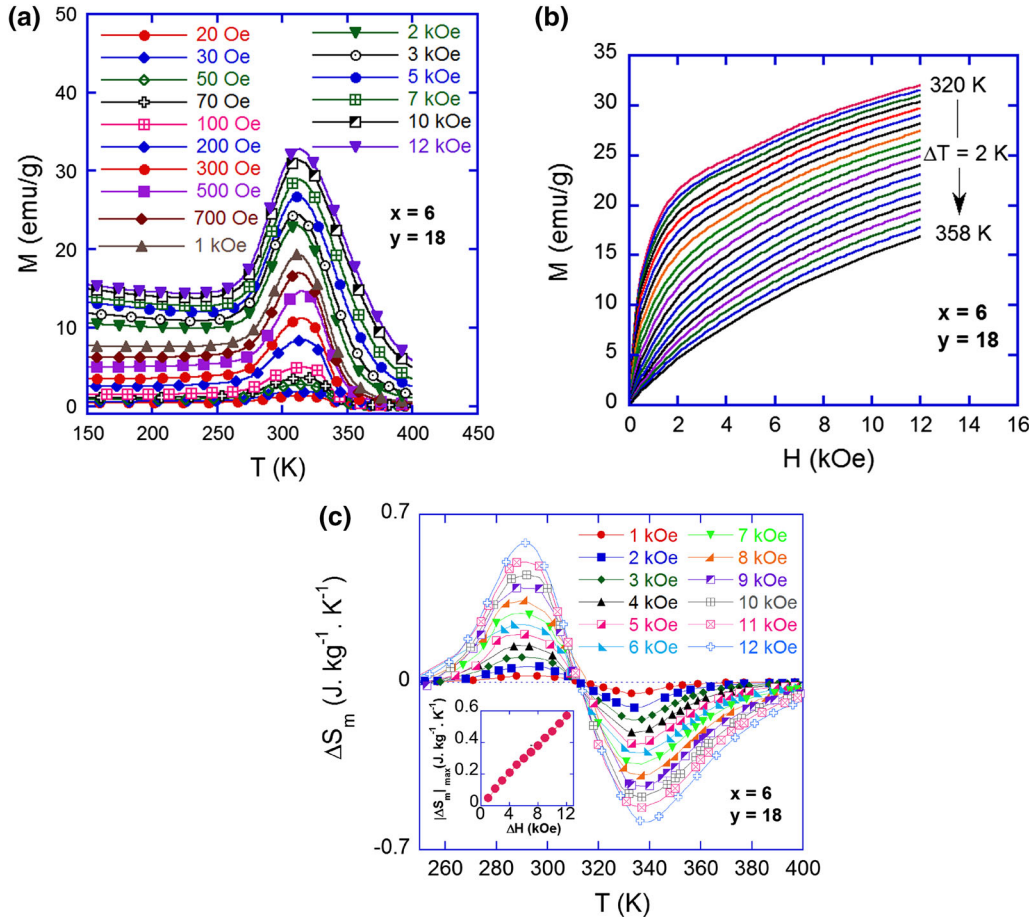


Fig. 4. $M(T)$ in various magnetic fields (a), $M(H)$ at different temperatures (b) and temperature dependence of magnetic entropy change $\Delta S_m(T)$ in various magnetic field changes (c) of $\text{Ni}_{44}\text{Co}_6\text{Mn}_{32}\text{Al}_{18}$ alloy ribbon. The inset shows maximum magnetic entropy change $|\Delta S_m|_{\max}$ versus magnetic field change ΔH .

the samples with Co concentrations of 5% and 10%. The $M(T)$ curves of $\text{Ni}_{50-x}\text{Co}_x\text{Mn}_{31}\text{Al}_{19}$ ($y = 19$) ribbons (Fig. 3c) show that the T_C^A is strongly increased from ~ 291 K to ~ 408 K by increasing the Co concentration from 5% to 10%. The martensitic–austenitic transformation tends to disappear with a high concentration of Co ($x \geq 7$), except for the sample with $x = 9$. In general, the increase in Co concentration simultaneously enhances the saturation magnetization and Curie temperature of the alloy ribbons. The martensitic–austenitic transition depends on both the Co and Al concentrations. By choosing appropriate concentrations of Co and Al, the magnetic phase transition temperatures can be desirably controlled. The strong dependence of the Curie temperature on Co concentration can be explained by exchange interactions of atoms in the alloy. The substitution of Co for Ni enhances exchange interactions of Ni–Mn and Co–Mn. As for the martensitic–austenitic transition, the concentration of valence electrons, i.e. number of valence electrons per atom (e/a), in the alloy plays a crucial role. The concentration of valence electrons is very sensitive to the composition of the alloy. This is a reason for the influence of the martensitic–

austenitic transformation on both the Co and Al concentrations in the alloy ribbons.

Among the fabricated alloy ribbons, the $\text{Ni}_{44}\text{Co}_6\text{Mn}_{32}\text{Al}_{18}$ sample shows both types of magnetic phase transitions around room temperature. Therefore, this sample was representatively selected to investigate its magnetocaloric effects. As is known, the magnetocaloric effect of a magnetic material can be assessed by its magnetic entropy change (ΔS_m). One way to determine the ΔS_m is through the use of the Maxwell equation:

$$\Delta S_m = \int_{H_1}^{H_2} \left(\frac{\partial M}{\partial T} \right)_H dH \quad (1)$$

From the experimental $M(T)$ curves (Fig. 4a), the corresponding $M(H)$ curves can be derived (Fig. 4b). Figure 4c presents the magnetic entropy change as a function of temperature, $\Delta S_m(T)$, of the $\text{Ni}_{44}\text{Co}_6\text{Mn}_{32}\text{Al}_{18}$ ribbon for various magnetic field changes ($\Delta H = 1\text{--}12$ kOe). One can see that the alloy ribbons exhibit both positive and negative magnetocaloric effects, with their maximum magnetic entropy

change larger than $0.6 \text{ J kg}^{-1} \text{ K}^{-1}$ in magnetic field change of 12 kOe. The maximum magnetic entropy change $|\Delta S_m|_{\max}$ increases with increasing magnetic field change ΔH (see the inset of Fig. 4c). The trend of $|\Delta S_m|_{\max}$ versus ΔH is quite linear and can be used to estimate $|\Delta S_m|_{\max}$ at higher values of magnetic field change ΔH .

CONCLUSION

The influence of Co and Al on the structure, magnetic properties and magnetocaloric effects of (Ni, Co)-Mn-(Sn, Al) alloy ribbons was investigated. Multi-crystalline phase behavior of the ribbons, including 4O, 14M, L1₀, B2, and 10M phases, was observed. All the ribbons exhibit soft magnetic feature with coercivity less than 50 Oe. The saturation magnetization and Curie temperature of the alloy strongly increased with increasing Co concentration. The amplitude and temperature of martensite–austenite phase transitions of the alloy clearly depend on both the Co and Al concentrations. Magnetic phase transitions in the alloy can be shifted to the room temperature region by adjusting the Co and Al concentrations. With appropriate concentrations of Co and Al, the ribbons possess both positive and negative MCE, with maximum magnetic entropy change larger than $0.6 \text{ J kg}^{-1} \text{ K}^{-1}$ in a magnetic field change of 12 kOe.

ACKNOWLEDGMENTS

This work was supported by the Vietnam Academy of Science and Technology under Grant Number VAST.CTVL.01/17-20. A portion of the work was carried out in the Key Lab for Electronic Materials and Devices and the Lab of Magnetism and Superconductivity, IMS, Vietnam. The work at Chungbuk National University was supported by the National Research Foundation of Korea through the Korea–Russia Joint Collaboration (No. 2017K1A3A1A49070064).

REFERENCES

- V.K. Pecharsky, K.A. Gschneidner, A.O. Pechasky, and A.M. Tishin, *Phys. Rev. B* 64, 144406 (2001).
- V. Franco, J.S. Blázquez, J.J. Ipus, J.Y. Law, L.M. Moreno-Ramírez, and A. Conde, *Prog. Mater. Sci.* 93, 112 (2018).
- V. Franco, J.S. Blázquez, B. Ingale, and A. Conde, *Annu. Rev. Mater. Res.* 42, 305 (2012).
- J. Sharma, A.A. Coelho, D.V.M. Repaka, R.V. Ramanujan, and K.G. Suresha, *J. Magn. Magn. Mater.* 487, 165307 (2019).
- A. Biswas, S. Chandra, T. Samanta, B. Ghosh, M.H. Phan, A.K. Raychaudhuri, I. Das, and H. Srikanth, *Phys. Rev. B* 87, 134420 (2013).
- A. Biswas, T.L. Phan, N.H. Dan, P. Zhang, S.C. Yu, H. Srikanth, and M.H. Phan, *Appl. Phys. Lett.* 103, 162410 (2013).
- T. Krenke, E. Duman, M. Acet, E.F. Wassermann, X. Moya, and L. Mañosa, *Nat. Mater.* 4, 450 (2005).
- A. Planes, L. Mañosa, and M. Acet, *J. Phys.* 21, 233201 (2009).
- R. Kainuma, W. Ito, R.Y. Umetsu, K. Oikawa, and K. Ishida, *Appl. Phys. Lett.* 93, 091906 (2008).
- T.L. Phan, P. Zhang, N.H. Dan, N.H. Yen, P.T. Thanh, T.D. Thanh, S.C. Yu, and M.H. Phan, *Appl. Phys. Lett.* 101, 202408 (2012).
- Y. Kim, E.J. Eun, J. Kim, K. Choi, W.B. Han, H.S. Kim, Y. Shon, and C.S. Yoon, *J. Alloys Compd.* 616, 66 (2014).
- M. Lyange, V. Khovaylo, R. Singh, S.K. Srivastava, R. Chatterjee, and L.K. Varga, *J. Alloys Compd.* 586, 218 (2013).
- O. Tegus, E. Brück, K.H. Buschow, and F.R. Boer, *Nature* 415, 6868 (2002).
- X. Zhang, B. Zhang, S. Yu, Z. Liu, W. Xu, and G. Liu, *Phys. Rev. B* 76, 132403 (2007).
- E. Bruck, *J. Appl. Phys.* 38, 381 (2005).
- K. Deepak and R.V. Ramanujan, *J. Alloys Compd.* 743, 494 (2018).
- X. Chen, V.B. Naik, R. Mahendiran, and R.V. Ramanujan, *J. Alloys Compd.* 618, 187 (2015).
- M. Kurniawan, A. Perrin, P. Xu, V. Keylin, and M. McHenry, *IEEE Magn. Lett.* 7, 6105005 (2016).
- A. Perrin, M. Sorescu, V. Keylin, D. Laughlin, and M. McHenry, *J. Mater.* 69, 2125 (2017).
- Y.B. Yang, X.B. Ma, X.G. Chen, J.Z. Wei, R. Wu, J.Z. Han, H.L. Du, C.S. Wang, S.Q. Liu, Y.C. Yang, Y. Zhang, and J.B. Yang, *J. Appl. Phys.* 111, 07A916 (2012).
- K.A. Gschneidner and V.K. Pecharsky, *Int. J. Refrig.* 31, 945 (2008).
- P. Felcher, J. Cable, and K. Wilkinson, *J. Phys. Chem. Solids* 24, 1663 (1963).
- F. Gejima, Y. Sutou, R. Kainuma, and K. Ishida, *Metall. Mater. Trans. A* 30, 2721 (1999).
- H.C. Xuan, F.H. Chen, P.D. Han, D.H. Wang, and Y.W. Du, *Intermetallics* 47, 31 (2014).
- M.V. Lyange, E.S. Barmina, and V.V. Khovaylo, *Mater. Sci. Found.* 81–82, 232 (2015).
- A.C. Paduani, A. Migliavacca, M.L. Sebben, J.D. Ardisson, M.I. Yoshida, S. Soriano, and M. Kalisz, *Solid State Commun.* 141, 145 (2007).
- T. Busgen, J. Feydt, R. Hassdorf, S. Thienhaus, and M. Moske, *Phys. Rev. B* 70, 014111 (2004).
- Y. Kim, W.B. Han, H.S. Kim, H.H. An, and C.S. Yoon, *J. Alloys Compd.* 557, 265 (2013).
- Y. Kim, S.J. Lee, W.B. Han, H.-S. Kim, H.H. An, and C.S. Yoon, *J. Appl. Phys.* 113, 17B102 (2013).
- X. Xu, W. Ito, M. Tokunaga, R.Y. Umetsu, R. Kainuma, and K. Ishida, *Mater. Trans.* 51, 1357 (2010).
- T. Krenke, E. Duman, M. Acet, E.F. Wassermann, X. Moya, L. Manosa, and A. Planes, *Nat. Mater.* 4, 450 (2005).
- T.L. Phan, N.H. Duc, N.H. Yen, P.T. Thanh, N.H. Dan, P. Zhang, and S.C. Yu, *IEEE Trans. Magn.* 48, 1381 (2012).
- D. Wu, S. Xue, J. Frenzel, G. Eggeler, Q. Zhai, and H. Zheng, *Mater. Sci. Eng. A* 534, 568 (2012).
- M.V. Lyange, V. Khovaylo, R. Singh, S.K. Srivastava, R. Chatterjee, and L.K. Varga, *J. Alloys Compd.* 586, 218 (2014).
- V. Khovaylo, M. Lyange, K. Skokov, O. Gutfleisch, R. Chatterjee, X. Xu, and R. Kainuma, *Mater. Sci. Forum* 738–739, 446 (2013).
- X. Xu, W. Ito, T. Kanomata, and R. Kainuma, *Entropy* 16, 1808 (2014).
- N. Kallel, S. Kallel, A. Hagaza, and M. Oumezzine, *Physica B* 404, 285 (2009).
- R.Y. Umetsu, A. Sheikh, W. Ito, B. Ouladdiaf, K.R.A. Ziebeck, T. Kanomata, and R. Kainuma, *Appl. Phys. Lett.* 98, 042507 (2011).
- R.Y. Umetsu, A. Fujita, W. Ito, T. Kanomata, and R. Kainuma, *J. Phys. Condens. Matter* 23, 326001 (2011).
- Z. Zhong, S. Ma, D. Wang, and Y. Du, *J. Mater. Sci. Technol.* 28, 193 (2012).